Computational Mechanics 29 (2002) 265–276 © Springer-Verlag 2002
DOI 10.1007/s00466-002-0339-6

Analytical and hybrid solutions of diffusion problems within arbitrarily shaped regions via integral transforms

L. A. Sphaier, R. M. Cotta

Abstract Linear diffusion problems defined within irregular multidimensional regions are analytically solved through integral transforms, requiring numerical routines only for integration purposes, when a general functional boundary representation is considered. Auxiliary one-dimensional eigenvalue problems mapping the irregular region are applied with an integral transformation procedure so that the original differential Sturm–Liouville system gives place to an algebraic eigenvalue problem. The exact analytical inversion formula is then employed to yield the desired potential, explicitly, at any point within the domain. To allow for improved flexibility and further applicability, the related integration is simplified through an approximate boundary representation using lines connecting user provided points instead of the former exact representation of the irregular bounds, which is particularly advantageous when a functional description of the boundaries is not available. A cylindrical region test case with known exact solution is considered, and treated as an irregular region in the Cartesian coordinates system. Convergence behavior and error analysis are carefully undertaken and illustrated.

Keywords Diffusion, Integral transformation, Analytical solution, Hybrid solution

List of symbols

$A_{h,l}$, $B_{h,l}$, $C_{h,l}$, $C^*_{h,l}$, $D_{h,l}$, $G_{h,l}$, $M_{h,l}$	matrix coefficients
b	maximum radius in test case
B	boundary differential operator
d, k, w, P	general diffusion problem parameters
$\bar{f}_i$	transformed initial condition
$f^*_{j,m}$	integral coefficient of transformed initial condition
$\bar{g}_i$	transformed non-homogeneous terms
$\mathbf{I}$	identity matrix
$\mathbf{n}$	boundary surface normal vector
N_i	norms of original eigenfunctions
N	truncation order
r, t, x, y, z	independent variables: radius, time, and Cartesian coordinates
R, X, Y	dimensionless independent variables
T	dependent variable: temperature
T_0	initial temperature
$\bar{T}_i$	transformed potentials
w^*, w_x, w_y, w_z	weighting functions
$\mathbf{x}$	position vector
$\tilde{X}_j$, $\tilde{Y}_m$, $\tilde{Z}_p$	normalized one-dimensional auxiliary eigenfunctions
x_0, x_1, y_0, y_1, z_0, z_1	domain bounds for Cartesian coordinate system
x^*_v	approximate boundary-representation x-points
y^v_0, y^v_1	approximate boundary-representation y-limits
$v_{\max}$	number of x-divisions required for approximate boundary description
$u_{\max}$	number of x-divisions in each 45° segment of test case circular bound

Greek symbols

α	thermal diffusivity
α_s, β_s	original eigenproblem boundary condition parameters
α^v_0, α^v_1, β^v_0, β^v_1	linear approximate boundary-representation coefficients
γ_m, λ_j	eigenvalues of auxiliary one-dimensional eigenproblems
Θ	dimensionless temperature
μ or μ_i	eigenvalues of original Sturm-Liouville problem
ν	Bessel function order in exact solution of test case
ϕ	independent variable: angle in the cylindrical coordinate system
ϕ_0	maximum angle in test case
Ψ or Ψ_i	original eigenfunctions
$\bar{\Psi}_{j,m,p}$ or $\bar{\Psi}_h$	transformed original eigenfunctions, from Sturm-Liouville problem
$\tilde{\Omega}_{j,m,p}$ or $\tilde{\Omega}_h$	auxiliary eigenfunctions
τ	dimensionless time

Received: 17 May 2001 / Accepted: 29 May 2002

L. A. Sphaier, R. M. Cotta (✉)
Laboratory of Transmission and Technology of Heat-LTTC,
Mechanical Engineering Department-EE/COPPE,
Universidade Federal do Rio de Janeiro-UFRJ,
Cidade Universitária-Cx. Postal 68503 Rio de Janeiro,
RJ 21945-970, Brazil
e-mail: renatocotta@hotmail.com

The authors would like to acknowledge the financial support provided by CNPq, CTPETRO, FAPERJ, and PRONEX, in Brazil.

Subscripts

i	original eigenproblem index
j, k, m, n, p	multiple eigenseries indices
h, l	single summation indices

1 Introduction

The last two decades were particularly fruitful in the advancement of numerical methods for diffusion and convection-diffusion problems, especially in their flexibilization towards the treatment of general multidimensional domain representations. While a lot is yet to be accomplished in terms of algorithm optimization and automatic stability and error control, it can be declared that the classical discrete approaches are nowadays capable of handling almost any complex geometric configuration, either through direct domain decomposition and discretization and/or physical domain transformation into computationally simpler representations. A rather complete compilation of such developments is presented in [1].

At the same time that the numerical methods and their commercial implementations evolve into more flexible and general tools, the requirements on validation and error analysis become more severe. Benchmarks on irregular geometries are somehow rare, due to inherent difficulties in the exact solution of such class of problems through the traditional analytical approaches. In this sense, and mainly towards this purpose, there is an open avenue for developments on hybrid methodologies, which may bring some diversity in terms of reference results for co-validation exercises. Besides, although eventually not with the same flexibility as in comparison with purely discrete schemes, hybrid paths may lead to more robust and accurate solution strategies in certain classes of problems.

Within this context, there has been a number of contributions on the analytical or semi-analytical treatment of diffusion and/or convection-diffusion within irregular geometries, in different physical areas [2–9], to mention a few.

One such alternative for the solution of partial differential equations within irregular regions has been progressively advanced through the so-called generalized integral transform technique, (GITT) [10–13]. Since 1989, a number of contributions have appeared in the integral transform solution of elliptic and parabolic diffusion problems within irregularly shaped domains [14–20]. All these contributions have in common the procedure of directly integral transforming the original partial differential system, starting from chosen one-dimensional eigenvalue problems which carry the information on the irregular shape through their own domain bounds, written as functions of the coordinate variables. These solutions have extended the available database on error controlled solutions of diffusion and convection-diffusion within more general domains, due to inherent capabilities of the integral transform approach in working within user prescribed accuracy targets.

More recently, in [21], this solution path was extended to directly handle multidimensional eigenvalue problems, and offer reliable estimates of eigenvalues and related quantities for certain classes of irregular domains. The extension of this analysis to the computation of the potential field itself, is now a straightforward task and particularly computationally effective for linear problems, when the integral transformation procedure yields decoupled ordinary differential equations for the transformed potentials, and the inversion formula provides a fully analytical solution for the original potential in all independent variables. Nevertheless, the approach is similarly applicable to nonlinear situations, as previously considered [19, 20].

The present contribution is thus intended to demonstrate this capability of exact solution of linear diffusion problems within irregular domains. But most important, we here introduce an approximate boundary-representation strategy for the cases when the boundary limits are provided only as points in space, which may also be used as a computational effort reduction alternative even for those cases when an exact closed form boundary functional description is offered. Such aspect has not been considered in previous contributions on this type of approach, and significantly adds to improve flexibility and applicability of the proposed method.

The analysis was performed using mixed symbolic-numerical computation [22], developing a computer code that includes the analytic derivations, numerical evaluations and graphics. Symbolical computation indeed facilitates the analysis and derivation tasks, and other software packages could also have been employed; nevertheless, such class of problems could still be handled by hand derivation at the cost of an increased developer effort.

A test case of known exact solution, related to heat conduction in a portion of a cylindrical region, is then employed to verify and validate the solution methodology and the symbolic-numerical computational implementation.

2 Solution methodology

One considers linear diffusion of the potential $T(\mathbf{x}, t)$ within an arbitrarily shaped region $\mathcal{V}$ with boundary surface $\mathcal{S}$, formulated as:

$$w(\mathbf{x})\frac{\partial T}{\partial t} = \nabla \cdot (k(\mathbf{x})\nabla T) - \mathrm{d}(\mathbf{x})T + P(\mathbf{x}, t), \quad \text{for } \mathbf{x} \in \mathcal{V} \text{ and } t > 0 \ , \tag{1a}$$

with the initial and boundary conditions:

$$T(\mathbf{x}, 0) = f(\mathbf{x}), \quad \text{for } \mathbf{x} \in \mathcal{V} \tag{1b}$$

and

$$BT(\mathbf{x}, t) = \phi(\mathbf{x}, t), \quad \text{for } \mathbf{x} \in \mathcal{S} \ , \tag{1c}$$

where the boundary operator is defined by

$$B = \alpha_s(\mathbf{x}) + \beta_s(\mathbf{x})k(\mathbf{x})\frac{\partial}{\partial \mathbf{n}}, \quad \text{with } \mathbf{x} \in \mathcal{S} \tag{1d}$$

and $\mathbf{n}$ is the outward drawn normal vector to surface $\mathcal{S}$.

The integral transform method in its classical sense [23] can be readily invoked to produce a formal exact solution to problem(1) above, based on the appropriate eigenfunction expansion in the following form:

$$T(\mathbf{x}, t) = \sum_{i=1}^{\infty} \frac{1}{N_i}\Psi_i(\mathbf{x})\bar{T}_i(t) \ , \tag{2a}$$

which is the corresponding inversion formula that reconstructs the original potential $T(\mathbf{x}, t)$ from the eigenfunctions $\Psi_i(\mathbf{x})$, the corresponding norms N_i and transformed potentials $\bar{T}_i(t)$, which are defined from the transformation

$$\bar{T}_i(t) = \int_{\mathcal{V}} w(\mathbf{x})\Psi_i(\mathbf{x})T(\mathbf{x}, t)\mathrm{d}v \ . \tag{2b}$$

The integral transformation of system (1a–c) results in a decoupled ODE system for the transformed potentials, solved as

$$\bar{T}_i(t) = \bar{f}_i e^{-\mu_i^2 t} + \int_0^t \bar{g}_i(t')e^{-\mu_i^2(t-t')}\mathrm{d}t' \ , \tag{3}$$

where μ_i's are the associated eigenvalues. The transformed initial condition, the norm and the transformed non-homogeneous terms are given respectively by

$$\bar{f}_i = \int_{\mathcal{V}} w(\mathbf{x})\Psi_i(\mathbf{x})f(\mathbf{x})\mathrm{d}v, \tag{4a, b}$$

$$N_i = \int_{\mathcal{V}} w(\mathbf{x})\Psi_i^2(\mathbf{x})\mathrm{d}v \ ,$$

$$\bar{g}_i(t) = \int_{\mathcal{V}} P(\mathbf{x}, t)\Psi_i(\mathbf{x})\mathrm{d}v + \int_{\mathcal{S}} \phi(\mathbf{x}, t)\left(\frac{\Psi_i(\mathbf{x}) - k(\mathbf{x})\frac{\partial\Psi_i(\mathbf{x})}{\partial\mathbf{n}}}{\alpha_s(\mathbf{x}) + \beta_s(\mathbf{x})}\right)\mathrm{d}s \ . \tag{4c}$$

Thus, to employ the above formal exact solution for a general arbitrarily shaped domain $\mathcal{V}$ in the realm of computation, one is left with the task of computationally solving the associated eigenvalue problem, given by

$$\nabla\cdot(k(\mathbf{x})\nabla\Psi(\mathbf{x})) + (\mu^2 w(\mathbf{x}) - \mathrm{d}(\mathbf{x}))\Psi(\mathbf{x}) = 0, \quad \mathbf{x}\in\mathcal{V} \tag{5a}$$

and

$$B\Psi(\mathbf{x}) = 0, \quad \mathbf{x}\in\mathcal{S} \ , \tag{5b}$$

to obtain the desired set of eigenfunctions $\Psi_i(\mathbf{x})$'s and the associated eigenvalues.

2.1 Expansion of the associated problem in terms of one-dimensional problems

In ref. [21], the same authors have proposed an integral transform solution to eigenvalue problems such as system (5a, b), defined in a certain class of irregular domains for which the bounding surfaces can be written as functions of the coordinate variables in an appropriate order. For instance, in the Cartesian coordinate system, domains defined by the following bounds:

$$x_0 \le x \le x_1, \quad y_0(x) \le y \le y_1(x), \quad z_0(x,y) \le z \le z_1(x,y) \ , \tag{6a–c}$$

where the limits on coordinate x are fixed, while the bounds on y are variable with coordinate x, and on the z variable may depend on both remaining coordinates. Under this representation, the integral transformation of problem (5a, b) into an algebraic eigensystem is as simple as in the case of regular domains [24].

According to the domain description introduced by Eqs. (6a–c), a normalized auxiliary eigenfunction, obtained by the solution of one-dimensional problems in each direction is constructed:

$$\tilde{\Omega}_h(\mathbf{x}) = \tilde{X}_j(x)\tilde{Y}_m(y;x)\tilde{Z}_p(z;x,y) \ , \tag{7a}$$

where, x and y are just parameters in the one-dimensional eigenvalue problem for $\tilde{Z}_p$, while x plays the role of a parameter in the solution of $\tilde{Y}_m$. These one-dimensional problems, recalling from [21], are special cases of the Sturm-Liouville problem that furnish a suitable eigenfunction basis for representing the original problem (5a, b). Thus, the following orthogonality relations are valid:

$$\int_{z_0(x,y)}^{z_1(x,y)} w_z(z)\tilde{Z}_p(z;x,y)\tilde{Z}_q(z;x,y)\mathrm{d}z = \delta_{p,q} \ , \tag{8a}$$

$$\int_{y_0(x)}^{y_1(x)} w_y(y)\tilde{Y}_m(y;x)\tilde{Y}_n(y;x)\mathrm{d}y = \delta_{m,n} \ , \tag{8b}$$

$$\int_{x_0}^{x_1} w_x(x)\tilde{X}_j(x)\tilde{X}_k(x)\mathrm{d}x = \delta_{j,k} \ , \tag{8c}$$

where w_x, w_y and w_z are the individual weighting functions related to each problem and the δ's are Kroneker Delta functions, i.e.

$$\delta_{i,j} = \begin{cases} 1, & \text{for } i = j \\ 0, & \text{for } i \ne j \end{cases} \ . \tag{9}$$

Based on the relations (8a–c), and provided the integration regarding the transformation process follows the appropriate order, initiating with the integration in the z-direction, followed by the y and finally the x coordinate, the global orthogonality property is readily satisfied:

$$\int_{\mathcal{V}} w^*(\mathbf{x})\tilde{\Omega}_h(\mathbf{x})\tilde{\Omega}_l(\mathbf{x})\mathrm{d}v = \delta_{h,l} \ , \tag{10}$$

where the volume integral needs to be conveniently written as a triple integral, with the following integration order

$$\int_{\mathcal{V}} \bullet\,\mathrm{d}v = \int_{x_0}^{x_1}\int_{y_0(x)}^{y_1(x)}\int_{z_0(x,y)}^{z_1(x,y)} \bullet\,\mathrm{d}z\,\mathrm{d}y\,\mathrm{d}x \tag{11}$$

and the global weighting function must be the product of the individual weighting functions in the one-dimensional problems:

$$w^*(x,y,z) = w_x(x)w_y(y)w_z(z) \ . \tag{12}$$

The index l is introduced in (10) to indicate different multidimensional eigenfunctions, just as the one-dimensional indices in (8a–c). Furthermore, the index h is related to the one-dimensional indices j, m and p through an appropriate computational combination and similarly is l, as outlined by the following relations:

$$\begin{aligned} &j, m, p \rightarrow h, \\ &k, n, q \rightarrow l \ . \end{aligned} \tag{13}$$

Once the global orthogonality property is provided, an adequate integral transform pair can be established:

$$\text{inverse} \Longrightarrow \Psi(\mathbf{x}) = \sum_{h=1}^{\infty} \tilde{\Omega}_h(\mathbf{x}) \bar{\Psi}_h \ , \tag{14a}$$

$$\text{transform} \Longrightarrow \bar{\Psi}_h = \int_{\mathcal{V}} w^*(\mathbf{x}) \tilde{\Omega}_h(\mathbf{x}) \Psi(\mathbf{x}) \mathrm{d}v \ . \tag{14b}$$

Or, using the multiple series representation, through the relations (13):

$$\begin{aligned} \Psi(\mathbf{x}) &= \Psi(x, y, z) \\ &= \sum_{j=1}^{\infty} \sum_{m=1}^{\infty} \sum_{p=1}^{\infty} \tilde{X}_j(x) \tilde{Y}_m(y; x) \tilde{Z}_p(z; x, y) \bar{\Psi}_{j,m,p} \end{aligned} \tag{15a}$$

and

$$\begin{aligned} \bar{\Psi}_{j,m,p} = \int_{x_0}^{x_1} \int_{y_0(x)}^{y_1(x)} \int_{z_0(x,y)}^{z_1(x,y)} &(w^*(x, y, z) \tilde{X}_j(x) \\ &\times \tilde{Y}_m(y; x) \tilde{Z}_p(z; x, y) \Psi(x, y, z)) \mathrm{d}z \, \mathrm{d}y \, \mathrm{d}x \ . \end{aligned} \tag{15b}$$

2.2 Integral transform of the associated problem

The integral transformation of problem (5a, b), is started by applying the integral operator $\int_{\mathcal{V}} \bullet \tilde{\Omega}_h(\mathbf{x}) \mathrm{d}v$ to Eq. (5a). The inversion formula (14a) is then substituted to produce the following system of coupled algebraic equations:

$$\begin{aligned} \sum_{l=1}^{\infty} \Bigg\{ &\int_{\mathcal{V}} \tilde{\Omega}_h(\mathbf{x}) \nabla \cdot (k(\mathbf{x}) \nabla \tilde{\Omega}_l(\mathbf{x})) \mathrm{d}v \\ &+ \mu^2 \int_{\mathcal{V}} w(\mathbf{x}) \tilde{\Omega}_h(\mathbf{x}) \tilde{\Omega}_l(\mathbf{x}) \mathrm{d}v \\ &- \int_{\mathcal{V}} \mathrm{d}(\mathbf{x}) \tilde{\Omega}_h(\mathbf{x}) \tilde{\Omega}_l(\mathbf{x}) \mathrm{d}v \Bigg\} \bar{\Psi}_l = 0 \ , \end{aligned} \tag{16}$$

for $h = 1, 2, \ldots, \infty$. Again, when the inversion formula is employed, l is used to distinguish from the index h, already present in the transformed system.

Now, one can write the algebraic system (16) in matrix form:

$$\left([\mathbf{A}] + \mu^2 [\mathbf{B}] - [\mathbf{D}]\right) \{\bar{\mathbf{\Psi}}\} = 0 \ , \tag{17}$$

where the involved quantities are given by

$$[\mathbf{A}] = A_{h,l} = \int_{\mathcal{V}} \tilde{\Omega}_h(\mathbf{x}) \nabla \cdot (k(\mathbf{x}) \nabla \tilde{\Omega}_l(\mathbf{x})) \mathrm{d}v \ , \tag{18a}$$

$$[\mathbf{B}] = B_{h,l} = \int_{\mathcal{V}} w(\mathbf{x}) \tilde{\Omega}_h(\mathbf{x}) \tilde{\Omega}_l(\mathbf{x}) \mathrm{d}v \ , \tag{18b}$$

$$[\mathbf{D}] = D_{h,l} = \int_{\mathcal{V}} d(\mathbf{x}) \tilde{\Omega}_h(\mathbf{x}) \tilde{\Omega}_l(\mathbf{x}) \mathrm{d}v \ , \tag{18c}$$

$$\{\bar{\mathbf{\Psi}}\} = \bar{\Psi}_l = \{\bar{\Psi}_1, \bar{\Psi}_2, \ldots\}^{\mathrm{T}} \ . \tag{18d}$$

The eigenvalues μ_i's are obtained by the computation of the square root of each eigenvalue of matrix $[\mathbf{M}]$, defined as:

$$[\mathbf{M}] = M_{h,l} = [\mathbf{B}]^{-1} ([\mathbf{D}] - [\mathbf{A}]) \ . \tag{19}$$

And the sets of coefficients $\bar{\Psi}_h$ associated with the eigenvalues μ_i's are given by the eigenvectors of $[\mathbf{M}]$. By substituting (14a) in (4a, b) one can easily derive an expression for the norms N_i in terms of the matrix and vector quantities available after the solution of (17):

$$N_i = \left([\mathbf{B}] \{\bar{\mathbf{\Psi}}\}\right) \cdot \{\bar{\mathbf{\Psi}}\} \ . \tag{20}$$

The reader should notice that once the orthogonality property of the auxiliary eigenfunctions $\tilde{\Omega}_h(\mathbf{x})$ is satisfied, if $w^* = w$ holds, $[\mathbf{B}]$ is reduced to the identity matrix and therefore,

$$M_{h,l} = D_{h,l} - A_{h,l} \quad \text{and} \quad N_i = \{\bar{\mathbf{\Psi}}\} \cdot \{\bar{\mathbf{\Psi}}\} \ . \tag{21a, b}$$

Now an important consideration regarding the transformation process described in the previous steps must be analyzed, related to the employment of Green's formulas, for the substitution of the diffusive term in transformed associated eigenvalue problem. We recall Green's first identity:

$$\begin{aligned} &\int_{\mathcal{V}} \tilde{\Omega}_h(\mathbf{x}) \nabla \cdot (k(\mathbf{x}) \nabla \Psi(\mathbf{x})) \mathrm{d}v \\ &\quad + \int_{\mathcal{V}} k(\mathbf{x}) (\nabla \tilde{\Omega}_h(\mathbf{x})) \cdot (\nabla \Psi(\mathbf{x})) \mathrm{d}v \\ &\equiv \int_{\mathcal{S}} k(\mathbf{x}) \tilde{\Omega}_h(\mathbf{x}) (\nabla \Psi(\mathbf{x})) \cdot \mathbf{n} \, \mathrm{d}s \end{aligned} \tag{22}$$

The inversion formula (14a) is then substituted in (22) yielding

$$([\mathbf{A}] + [\mathbf{G}]) \{\bar{\mathbf{\Psi}}\} = [\mathbf{C}] \{\bar{\mathbf{\Psi}}\} \tag{23a}$$

In a similar fashion, Green's second identity gives:

$$([\mathbf{A}] - [\mathbf{A}]^{\mathrm{T}}) \{\bar{\mathbf{\Psi}}\} = ([\mathbf{C}] - [\mathbf{C}]^{\mathrm{T}}) \{\bar{\mathbf{\Psi}}\} = [\mathbf{C}^*] \{\bar{\mathbf{\Psi}}\} \ , \tag{23b}$$

where $[\mathbf{A}]^{\mathrm{T}}$ and $[\mathbf{C}]^{\mathrm{T}}$ are the transposes of $[\mathbf{A}]$ and $[\mathbf{C}]$, respectively. The matrices $[\mathbf{G}]$, $[\mathbf{C}]$ and $[\mathbf{C}^*]$ are given by:

$$[\mathbf{G}] = G_{h,l} = \int_{\mathcal{V}} (\nabla \tilde{\Omega}_h(\mathbf{x})) \cdot (k(\mathbf{x}) \nabla \tilde{\Omega}_l(\mathbf{x})) \mathrm{d}v \ , \tag{24a}$$

$$[\mathbf{C}] = C_{h,l} = \int_{\mathcal{S}} k(\mathbf{x})\left(\tilde{\mathbf{\Omega}}_h(\mathbf{x})\nabla\tilde{\mathbf{\Omega}}_l(\mathbf{x})\right)\cdot\mathbf{n}\,ds \ , \tag{24b}$$

$$[\mathbf{C}^*] = C^*_{h,l} = \int_{\mathcal{S}} k(\mathbf{x})(\tilde{\mathbf{\Omega}}_h(\mathbf{x})\nabla\tilde{\mathbf{\Omega}}_l(\mathbf{x}) - \tilde{\mathbf{\Omega}}_l(\mathbf{x})\nabla\tilde{\mathbf{\Omega}}_h(\mathbf{x}))\cdot\mathbf{n}\,ds \ . \tag{24c}$$

Based on an analysis of the former matrices, it can be easily shown that if $[\mathbf{C}^*]$ is a null matrix and $\{\mathbf{\Psi}\}$ is a non-null vector, $[\mathbf{A}]$ is symmetric. This remark is very useful while implementing the computational solution, because a considerable amount of computational effort can be spared by calculating only half of the off-diagonal coefficients when generating this matrix. Thus, for the sake of this simplification, it is necessary that $C^*_{h,l} = 0$, i.e. the surface integrals in (24c) vanish. As demonstrated in [25], if the global multidimensional auxiliary eigenfunctions satisfy $B\tilde{\mathbf{\Omega}}_h(\mathbf{x}) = 0$ for $\mathbf{x}\in\mathcal{S}$, then this requirement is fulfilled. It can also be inferred for the cases with $C_{h,l} = 0$, i.e. when the integrals in (24b) are null, if $\{\mathbf{\Psi}\}$ is a non-null vector, then $[\mathbf{A}] = -[\mathbf{G}]$.

The interested reader is referred to the contributions [21] and [25], which provide further details on the analysis and computational implementation of these integral transform solutions of eigenvalue problems within irregular domains.

3 Test case

As a test case of the proposed methodology, the heat or mass diffusion problem in a portion of a circular region is considered (Fig. 1), which yields the following transient problem in the cylindrical coordinate system:

$$\frac{1}{\alpha}\frac{\partial T}{\partial t} = \frac{1}{r}\frac{\partial}{\partial r}\left(r\frac{\partial T}{\partial r}\right) + \frac{1}{r^2}\frac{\partial^2 T}{\partial \phi^2},$$

$$\text{in} \quad 0 \le r \le b, \quad 0 \le \phi \le \phi_0$$

$$\text{and} \quad t > 0 \ , \tag{25a}$$

$$T = 0, \quad \text{at} \quad r = b, \quad \phi = 0, \quad \text{and} \quad \phi = \phi_0 \ , \tag{25b}$$

$$T = T_0, \quad \text{for} \quad t = 0, \quad \text{in} \quad 0 \le r \le b \quad \text{and} \quad 0 \le \phi \le \phi_0 \ , \tag{25c}$$

which is solved through separation of variables [26] to yield

$$T(r,\phi,t) = \frac{8T_0}{b^2\phi_0}\sum_{p=1}^{\infty}\sum_{v} e^{-\alpha\beta_p^2 t}\frac{J_v(\beta_p r)}{J_v'^2(\beta_p r)}\frac{\sin(v\phi)}{v} \times \int_{r'=0}^{b} J_v(\beta_p r')\mathrm{d}r' \ , \tag{26a}$$

where the β_p's are the roots of

$$J_v(\beta_p b) = 0 \tag{26b}$$

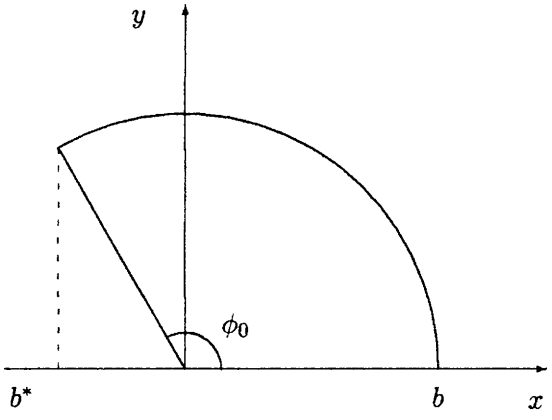

Fig. 1. Geometry and coordinate system for test case

and the v's are given by

$$v = \frac{(2n-1)\pi}{\phi_0}, \quad \text{for} \quad n = 1,2,3,\ldots \tag{26c}$$

This problem will provide a test case once one considers its representation in the Cartesian coordinate system, interpreting the portion of the circular region as an irregular domain, bounded by:

$$x_0 \le x \le x_1 \quad \text{and} \quad y_0(x) \le y \le y_1(x) \ , \tag{27a, b}$$

where from the situation exhibited in Fig. 1:

$$x_0 = b^* = b\cos(\phi_0), \quad x_1 = b \ ,$$

$$y_0(x) = \begin{cases} x\tan(\phi_0) & \text{if } x < 0 \\ 0 & \text{if } x \ge 0 \end{cases}, \tag{27c, d}$$

$$y_1(x) = \sqrt{b^2 - x^2} \ .$$

The transient heat conduction problem is then rewritten as

$$\frac{1}{\alpha}\frac{\partial T}{\partial t} = \frac{\partial^2 T}{\partial x^2} + \frac{\partial^2 T}{\partial y^2}, \quad \text{in} \quad y_0(x) \le y \le y_1(x),$$

$$\text{for} \quad x_0 \le x \le x_1 \quad \text{and} \quad t > 0 \ , \tag{28a}$$

$$T = 0, \quad \text{at} \quad x = x_0 \quad \text{and} \quad x = x_1 \ , \tag{28b}$$

$$T = 0, \quad \text{at} \quad y = y_0(x) \quad \text{and} \quad y = y_1(x),$$

$$\text{for} \quad x_0 \le x \le x_1 \ , \tag{28c}$$

$$T = T_0, \quad \text{for} \quad t = 0, \quad \text{in} \quad y_0(x) \le y \le y_1(x),$$

$$\text{for} \quad x_0 \le x \le x_1 \ . \tag{28d}$$

The exact solution of problem (28a–d) is given by:

$$T(x,y,t) = \sum_{i=1}^{\infty} \mathrm{e}^{-\alpha\mu_i^2 t}\frac{\Psi_i(x,y)\bar{f}_i}{N_i} \ , \tag{29}$$

where the related eigenvalue problem is

$$\frac{\partial^2\Psi(x,y)}{\partial x^2} + \frac{\partial^2\Psi(x,y)}{\partial y^2} + \mu^2\Psi(x,y) = 0,$$

$$\text{in} \quad y_0(x) \le y \le y_1(x), \quad \text{for} \quad x_0 \le x \le x_1 \ , \tag{30a}$$

$$\Psi(x,y)=0, \quad \text{at} \quad y=y_0(x) \quad \text{and} \quad y=y_1(x),$$
$$\text{for} \quad x_0 \le x \le x_1 \ , \tag{30b}$$
$$\Psi(x,y)=0, \quad \text{at} \quad x=x_0 \quad \text{and} \quad x=x_1 \ . \tag{30c}$$

The next task is to obtain the solution of the eigenvalue problem (30a–b) from the irregular domain representation proposed for the circular region portion. The auxiliary one-dimensional eigenvalue problems are given by:

$$\frac{\mathrm{d}^2\tilde{X}_j}{\mathrm{d}x^2}+\lambda_j^2\tilde{X}_j=0, \quad \text{in} \quad x_0 \le x \le x_1 \ , \tag{31a}$$
$$\tilde{X}_j(x_0)=\tilde{X}_j(x_1)=0 \ , \tag{31b}$$

and

$$\frac{\mathrm{d}^2\tilde{Y}_m}{\mathrm{d}y^2}+\gamma_m^2\tilde{Y}_m=0, \quad \text{in} \quad y_0(x) \le y \le y_1(x),$$
$$\text{for} \quad x_0 \le x \le x_1 \ , \tag{32a}$$
$$\tilde{Y}_m(y_0(x))=\tilde{Y}_m(y_1(x))=0, \quad \text{for} \quad x_0 \le x \le x_1 \ , \tag{32b}$$

which upon using the normalization integrals

$$\int_{x_0}^{x_1}\tilde{X}_j^2(x)\mathrm{d}x=1 \quad \text{and} \quad \int_{y_0(x)}^{y_1(x)}\tilde{Y}_m^2(y;x)\mathrm{d}y=1 \ , \tag{33a, b}$$

are readily solved to yield

$$\tilde{X}_j(x)=\frac{\sqrt{2}\sin(\lambda_j(x-x_0))}{\sqrt{x_1-x_0}} \quad \text{and}$$
$$\tilde{Y}_m(y;x)=\frac{\sqrt{2}\sin(\gamma_m(y-y_0(x)))}{\sqrt{y_1(x)-y_0(x)}} \ , \tag{34a, b}$$

and the associated equations for the eigenvalues:

$$\sin(\lambda_j(x_1-x_0))=0, \quad \text{or} \quad \lambda_j=\frac{j\pi}{x_1-x_0}$$
$$\text{with} \quad j=1,2,3,\ldots \tag{35a}$$
$$\sin(\gamma_m(y_1(x)-y_0(x)))=0, \quad \text{or} \quad \gamma_m=\frac{m\pi}{y_1(x)-y_0(x)}$$
$$\text{with} \quad m=1,2,3,\ldots \tag{35b}$$

Note that for the presented test case, $[\mathbf{D}]$ is null matrix due to the value of $\mathrm{d}(\mathbf{x})$. Besides, the Dirichlet boundary conditions considered in the one-dimensional eigenproblems not only readily satisfy the relation $B\tilde{\Omega}_h(\mathbf{x})=0$, but also lead to $C_{h,l}=0$. In addition, as $w(\mathbf{x})=1$ and $w_x(x)=w_y(y)=1$, the relations (21 a, b) also hold. Thus, the expressions for the matrix coefficients are simplified, with $M_{h,l}$ given by $M_{h,l}=-A_{h,l}=G_{h,l}$ and evaluated from Eq. (24a).

3.1
Computational solution procedure

To initiate the computational solution process, one starts by evaluating the matrix coefficients, for this test case given by:

$$M_{h,l} \rightleftharpoons M_{j,m,k,n}=\int_{x_0}^{x_1}\int_{y_0(x)}^{y_1(x)}\nabla(\tilde{X}_j(x)\tilde{Y}_m(y;x)) \cdot \nabla(\tilde{X}_k(x)\tilde{Y}_n(y;x))\mathrm{d}y\,\mathrm{d}x \ , \tag{36}$$

where the gradient operator is defined in the Cartesian coordinate system. Note also that for the matrix assembly a proper index combination is required, as shown by (13). Index grouping procedures, denominated reordering schemes, are discussed in [27]. The reordering scheme adopted in this work is explained with details in [21].

Once the matrix assembly is completed, the transformed coefficients $\bar{\Psi}_h=\bar{\Psi}_{j,m}$ are obtained through the solution of the algebraic system (17). Note that (17) will provide eigenvectors $\{\bar{\Psi}\}$, each one associated with an eigenvalue μ_i, to be employed in the reconstruction of the respective eigenfunction $\Psi_i(x,y)$, by means of the inversion formula:

$$\Psi_i(x,y)=\Psi(x,y)=\sum_{j=1}^{\infty}\sum_{m=1}^{\infty}\tilde{X}_j(x)\tilde{Y}_m(y;x)\bar{\Psi}_{j,m} \ . \tag{37a}$$

Finally, the solution for the desired temperature field is carried-out through Eq. (29), where the norm is evaluated from Eqs. (21a, b) and the transformed initial condition is calculated by:

$$\bar{f}_i=T_0\sum_{j=1}^{\infty}\sum_{m=1}^{\infty}\bar{f}_{j,m}^{*}\bar{\Psi}_{j,m} \ , \tag{37b}$$

with

$$\bar{f}_{j,m}^{*}=\int_{b^*}^{b}\tilde{X}_j(x)\left(\int_{y_0(x)}^{y_1(x)}\tilde{Y}_m(y;x)\mathrm{d}y\right)\mathrm{d}x \ . \tag{37c}$$

Note that the same index combination rules employed in the evaluation of $[\mathbf{M}]$ must be used throughout the computational process.

One must realize that the employment of a computational solution requires all infinite series formerly considered to be approximated by finite summations. This hence gives rise to a truncation error that diminishes as the number of summed terms increases. By these means, an effective user error-controlled solution can be achieved.

4
Approximate boundary-representation

Although elegant and exact, the previous solution strategy is somehow limited to domain descriptions in terms of functions as considered in (6a–c). Besides, the numerical integration task for a general functional boundary-description, as required in the evaluation of the matrix coefficients $M_{h,l}$, may eventually become prohibitive for most practical purposes. The major difficulty lies on the attempt of analytically integrating in the x-direction. While the in-

tegration in the y-direction is straightforward, it introduces the functions $y_0(x)$ and $y_1(x)$, and their derivatives, in the integrand of the following integral along the fixed bounds of the x-direction. For instance, for a general two-dimensional problem with Dirichlet boundary conditions, i.e. allowing any boundary functional representation ($y_0(x) \le y \le y_1(x)$ for $x_0 \le x \le x_1$), the matrix coefficients $M_{h,l} \rightleftharpoons M_{j,m,k,n}$, after integration in the y direction are given by:

$$\begin{aligned} M_{j,m,k,n} = {} & \frac{mn}{(x_1-x_0)^2(m+n)^2(m-n)^2} \\ & \times \int_{x_0}^{x_1} \frac{y_0'(x) - (-1)^{m+n} y_1'(x)}{(y_1(x)-y_0(x))^2} \\ & \times (2\pi(m+n)(m-n)[(j+k) \\ & \times \sin((\lambda_j - \lambda_k)(x-x_0)) \\ & + (k-j)\sin((\lambda_j+\lambda_k)(x-x_0))](y_1(x)-y_0(x)) \\ & + 8(m^2+n^2)(x_1-x_0)\sin(\lambda_j(x-x_0)) \\ & \times \sin(\lambda_k(x-x_0))\big(y_0'(x)-y_1'(x)\big)\big)\mathrm{d}x \ , \end{aligned} \tag{38a}$$

for $m \neq n$, and

$$\begin{aligned} M_{j,m,k,m} = {} & \lambda_j^2 \delta_{j,k} + \frac{1}{6(x_1-x_0)} \\ & \times \int_{x_{o-1}^*}^{x_o^*} \frac{\sin(\lambda_j(x-x_0))\sin(\lambda_k(x-x_0))}{(y_1(x)-y_0(x))^2} \\ & \times \Big(12\pi^2 m^2 + (4\pi^2 m^2+3)\Big(\big(y_0'(x)\big)^2 + \big(y_1'(x)\big)^2\Big) \\ & + 2(2\pi^2 m^2 - 3) y_0'(x) y_1'(x)\Big)\mathrm{d}x \ , \end{aligned} \tag{38b}$$

for $n = m$, as directly obtained from symbolic manipulation with the Mathematica system. The above integral formulas must be adapted for the cases where $y_0(x)$ and/or $y_1(x)$ demand a definition in steps, i.e. requiring different functional forms for different x-intervals. This is accomplished by permitting these integrals to be written as a sum of integrals over each of these x-intervals.

For certain simple functional forms $y_0(x)$ and $y_1(x)$, the integrals in the x-direction may also be analytically obtained, as discussed in [21]. Otherwise, the integrals (38a, b) are to be performed numerically, which could result in a substantial computational effort if a fully error controlled solution is being requested. To overcome this obstacle, the ideas already presented are further extended, allowing more general purpose and flexible integral transform solutions of diffusion problems within arbitrarily shaped domains.

One sufficiently simple and efficient alternative is to replace the functional representations, $y_0(x)$ and $y_1(x)$, by first order polynomials connecting user provided boundary points, or:

$$\begin{aligned} & y_0(x) \approx y_0^\nu(x) = \alpha_0^\nu x + \beta_0^\nu, \\ & y_1(x) \approx y_1^\nu(x) = \alpha_1^\nu x + \beta_1^\nu \\ & \quad \text{for } x_{\nu-1}^* < x < x_\nu^*, \quad \text{with } \nu = 1, 2, \ldots, \nu_{\max} \end{aligned} \tag{39a, b}$$

and the x-integrals are replaced by

$$\int_{x_0}^{x_1} \bullet \mathrm{d}x \to \sum_{\nu=1}^{\nu_{\max}} \int_{x_{\nu-1}^*}^{x_\nu^*} \bullet \mathrm{d}x \ , \tag{39c}$$

where $\nu_{\max}$ is the required number of divisions in the x-domain, according to the provided boundary points. The parameters α_0^ν, β_0^ν, α_1^ν and β_1^ν are constants comprising the linear interpolation. At the extremes of the x variable, one should obtain the relations $x_0^* = x_0$ and $x_{\nu_{\max}}^* = x_1$.

The resulting integrals of (38a, b) are then analytically evaluated through the Mathematica system, but not presented here due to space limitations. This approximate representation of the boundary functions can be made increasingly more accurate by including further boundary points and/or increasing the interpolation order (in general second or third order polynomials). It should also be clear that this strategy does not represent a discretization of the solution domain, and the final solution remains analytical and explicitly achievable at any domain position (x, y). Essentially, only the functional representation of the boundaries are being approximated for flexibility and computational performance improvement. Moreover, in practice, many domain configurations are not even available in a global functional form, and are in fact provided as a set of points in space.

5 Results and discussion

In this section the results are screened in tabular and graphical forms, allowing a concise convergence analysis to be carried out. Before presenting the results, the following non-dimensional variables should be introduced:

$$R = \frac{r}{b}, \quad X = \frac{x}{b}, \quad Y = \frac{y}{b}, \quad \Theta = \frac{T}{T_0}, \quad \tau = \frac{\alpha t}{b^2} \ . \tag{40}$$

The numerical results for the test case are hence exhibited as the non-dimensional temperature Θ for different times τ and positions (R, ϕ), within different domain configurations described by the geometric parameter ϕ_0.

To analyze the convergence behavior of Θ with the truncation order N, one starts by observing Table 1, where numerical results are presented for different geometric configurations. Four different points within the irregular domain are taken for each case, two of these at half the radius ($R = 1/2$) for $\phi = \phi_0/4$ and $\phi = 3\phi_0/4$. Similarly, the other two are taken at half the total angle ($\phi = \phi_0/2$) for $R = 1/4$ and $R = 3/4$.

Analyzing the results in Table 1 we note that the cases where single functions are used for describing the bounds $y_0(x)$ and $y_1(x)$, i.e. $\phi_0 = 90^\circ$ and $\phi_0 = 180^\circ$, present better convergence rates, having an average of four or more converged significant figures with $N = 500$ and slightly less for N as low as $N = 100$. For the case of $\phi_0 = 45^\circ$ the solution presents an average of three converged significant figures for a truncation order $N = 500$. This worsening is most likely due to the sharp edges en-

Table 1. Convergence analysis of temperature field for exact boundary-representation

N	$\tau = 10^{-2}$	$\tau = 10^{-1.5}$	$\tau = 10^{-1}$	N	$\tau = 10^{-2}$	$\tau = 10^{-1.5}$	$\tau = 10^{-1}$
$\phi_0 = 45°$							
$\phi = 11.25°$, $R = 1/2$				$\phi = 22.5°$, $R = 1/4$			
20	0.458130	0.121747	0.002135	20	0.150806	0.021302	0.000357
40	0.462669	0.119793	0.002195	40	0.146935	0.020568	0.000358
60	0.468494	0.120884	0.002241	60	0.148340	0.021176	0.000373
80	0.464720	0.120636	0.002258	80	0.144920	0.020236	0.000358
100	0.461695	0.120274	0.002259	100	0.146014	0.020297	0.000361
150	0.463051	0.120431	0.002274	150	0.145807	0.020450	0.000365
200	0.463243	0.120508	0.002281	200	0.144814	0.020256	0.000362
250	0.463048	0.120500	0.002284	250	0.145274	0.020283	0.000363
300	0.463197	0.120495	0.002286	300	0.145451	0.020325	0.000364
350	0.463221	0.120551	0.002288	350	0.145288	0.020295	0.000364
400	0.463187	0.120554	0.002290	400	0.145288	0.020295	0.000364
450	0.463359	0.120607	0.002292	450	0.145416	0.020325	0.000365
500	0.463326	0.120593	0.002292	500	0.145437	0.020336	0.000365
exact	0.463283	0.120644	0.002302	exact	0.145344	0.020317	0.000366
$\phi = 22.5°$, $R = 3/4$				$\phi = 33.75°$, $R = 1/2$			
20	0.814555	0.237871	0.004250	20	0.484384	0.124348	0.002179
40	0.828233	0.249496	0.004696	40	0.465609	0.120284	0.002205
60	0.832825	0.251672	0.004791	60	0.466434	0.120878	0.002241
80	0.829325	0.253123	0.004869	80	0.463234	0.120532	0.002256
100	0.828759	0.253957	0.004905	100	0.462315	0.120072	0.002255
150	0.830538	0.255603	0.004963	150	0.462468	0.120197	0.002269
200	0.829534	0.255801	0.004979	200	0.463643	0.120546	0.002281
250	0.829366	0.256070	0.004992	250	0.463550	0.120557	0.002285
300	0.828849	0.256137	0.004998	300	0.463235	0.120501	0.002286
350	0.828384	0.256151	0.005002	350	0.463024	0.120478	0.002287
400	0.828349	0.256206	0.005006	400	0.463178	0.120527	0.002289
450	0.828263	0.256245	0.005009	450	0.463314	0.120565	0.002291
500	0.828006	0.256233	0.005010	500	0.463404	0.120580	0.002292
exact	0.828653	0.256891	0.005043	exact	0.463283	0.120644	0.002302
$\phi_0 = 90°$							
$\phi = 22.5°$, $R = 1/2$				$\phi = 45°$, $R = 1/4$			
20	0.826410	0.467917	0.077092	20	0.619791	0.264787	0.043132
40	0.822662	0.467114	0.077127	40	0.622127	0.263828	0.042912
60	0.823553	0.467492	0.077187	60	0.622110	0.263720	0.042909
80	0.821810	0.467015	0.077140	80	0.622360	0.263955	0.042948
100	0.822716	0.467283	0.077183	100	0.622108	0.263829	0.042929
150	0.822122	0.467144	0.077173	150	0.622060	0.263830	0.042933
200	0.822500	0.467267	0.077191	200	0.622070	0.263843	0.042936
250	0.822584	0.467293	0.077197	250	0.621980	0.263818	0.042933
300	0.822594	0.467313	0.077202	300	0.622092	0.263854	0.042940
350	0.822553	0.467295	0.077199	350	0.622061	0.263843	0.042938
400	0.822519	0.467291	0.077199	400	0.622098	0.263858	0.042941
450	0.822453	0.467274	0.077197	450	0.622071	0.263854	0.042941
500	0.822462	0.467279	0.077198	500	0.622033	0.263839	0.042938
exact	0.822494	0.467296	0.077202	exact	0.622048	0.263844	0.042940
$\phi = 45°$, $R = 3/4$				$\phi = 67.5°$, $R = 1/2$			
20	0.911644	0.564892	0.095289	20	0.817741	0.469434	0.077304
40	0.909336	0.564142	0.095528	40	0.820751	0.466911	0.077110
60	0.910030	0.564482	0.095600	60	0.823013	0.467389	0.077189
80	0.910949	0.564741	0.095638	80	0.822266	0.467155	0.077158
100	0.910214	0.564629	0.095637	100	0.822643	0.467371	0.077204
150	0.910379	0.564640	0.095650	150	0.822541	0.467291	0.077192
200	0.910326	0.564644	0.095656	200	0.822375	0.467258	0.077191
250	0.910236	0.564623	0.095655	250	0.822536	0.467314	0.077201
300	0.910313	0.564646	0.095660	300	0.822506	0.467294	0.077198
350	0.910337	0.564647	0.095661	350	0.822473	0.467295	0.077200
400	0.910416	0.564671	0.095665	400	0.822465	0.467286	0.077198
450	0.910449	0.564686	0.095667	450	0.822520	0.467309	0.077203
500	0.910356	0.564656	0.095664	500	0.822504	0.467297	0.077201
exact	0.910395	0.564673	0.095668	exact	0.822494	0.467296	0.077202

Table 1. (Contd.)

N	$\tau = 10^{-2}$	$\tau = 10^{-1.5}$	$\tau = 10^{-1}$	N	$\tau = 10^{-2}$	$\tau = 10^{-1.5}$	$\tau = 10^{-1}$
$\phi_0 = 180^\circ$							
$\phi = 45^\circ$, $R = 1/2$				$\phi = 90^\circ$, $R = 1/4$			
20	0.983827	0.771779	0.270128	20	0.938984	0.668987	0.270744
40	0.990550	0.774497	0.270795	40	0.926255	0.671740	0.271693
60	0.988709	0.775870	0.271187	60	0.920694	0.672939	0.271959
80	0.985024	0.774672	0.271041	80	0.921199	0.673207	0.272012
100	0.988210	0.775399	0.271176	100	0.924347	0.674505	0.272326
150	0.987510	0.775182	0.271181	150	0.922976	0.673958	0.272217
200	0.987379	0.775181	0.271195	200	0.922779	0.673945	0.272228
250	0.987152	0.775082	0.271190	250	0.922718	0.673947	0.272245
300	0.986995	0.775039	0.271176	300	0.922921	0.673976	0.272248
350	0.986828	0.775005	0.271181	350	0.923044	0.674011	0.272257
400	0.987112	0.775070	0.271193	400	0.923014	0.674010	0.272253
450	0.987007	0.775055	0.271189	450	0.923021	0.674012	0.272261
500	0.986908	0.775023	0.271186	500	0.922983	0.674002	0.272257
exact	0.987003	0.775059	0.271199	exact	0.922900	0.673974	0.272256
$\phi = 90^\circ$, $R = 3/4$				$\phi = 135^\circ$, $R = 1/2$			
20	0.919546	0.619626	0.241925	20	0.983827	0.771779	0.270128
40	0.912565	0.623380	0.242406	40	0.990550	0.774497	0.270795
60	0.910628	0.625339	0.242992	60	0.988709	0.775870	0.271187
80	0.911339	0.625268	0.242959	80	0.985024	0.774672	0.271041
100	0.911620	0.625224	0.243028	100	0.988210	0.775399	0.271176
150	0.911476	0.625302	0.242987	150	0.987510	0.775182	0.271181
200	0.910173	0.624797	0.242857	200	0.987379	0.775181	0.271195
250	0.910717	0.625045	0.242915	250	0.987152	0.775082	0.271190
300	0.911011	0.625137	0.242951	300	0.986995	0.775039	0.271176
350	0.910806	0.625081	0.242946	350	0.986828	0.775005	0.271181
400	0.910768	0.625052	0.242937	400	0.987112	0.775070	0.271193
450	0.910713	0.625027	0.242928	450	0.987007	0.775055	0.271189
500	0.910704	0.625020	0.242923	500	0.986908	0.775023	0.271186
exact	0.910748	0.625046	0.242936	exact	0.987003	0.775059	0.271199

countered at the boundaries within $x_0 < x < x_1$, which result in a discontinuity on the derivatives of $y_0(x)$ and $y_1(x)$. Besides, the vector **n** cannot be defined for these points. Therefore, this result might be improved by making use of unit-step functions to define the y-limits at these points.

For an illustration of the graphical convergence, the case with $\phi_0 = 225^\circ$ and $\tau = 0.03$ is chosen. The graphics are presented in Fig. 2 for different truncation orders. The contours are lines of constant temperature, having the values $\Theta = 0.1, 0.3, 0.6, 0.8$ and 0.9. For the other values of ϕ_0 outlined in Table 1, a similar behavior is observed, with even better convergence rates (when considering the same value for τ). For smaller values of time the convergence rate also diminishes, due to the smaller damping factor in the time exponential, as observed in similar eigenseries solutions.

Again, confirming the observation on the effect of the sharp edges, it can be easily noted that the solution always worsens for points in the vicinity of those sharp edges or which have their x-coordinate near that of the described geometric singularity point.

To carry out a quantitative analysis of convergence rates for the approximate boundary-representation, one starts by increasing the number of boundary points for a fixed truncation order and comparing the results with the equivalent exact boundary-representation case. The points are scattered throughout the circular portion of the boundaries, preserving a constant angular spacing. One should remember that for these cases the solution is fully-analytical, and even the matrix coefficient integrals can be carried out by analytical means leading to expressions in terms of the well known cosine-integral and sine-integral functions.

The results are presented in Table 2 for two different non-dimensional times, $\tau = 10^{-2}$ and $\tau = 10^{-1.5}$, for the geometric configuration with $\phi_0 = 90^\circ$ ($\nu_{\max} = \infty$ refers to the exact, or continuous, boundary representation). Although only a limited set of results is presented, due to space limitations, it can be declared that a similar behavior is observed among all cases. We chose to present the results for a fixed angle at different radii, since the variation of the convergence rate while one approaches the approximated boundary can be analyzed. However, even for this few number of points along the radial direction, one can easily infer that the convergence rate (with respect to the number of boundary points/divisions) worsens as the approximated boundary is approached, which could be expected.

As mentioned for the exact boundary-representation, the described sharp edges occur in every point within the x limits for the approximate boundary-representation. Therefore, by employing higher order polynomials to interpolate the boundary points, ensuring the continuity of the first derivatives of the interpolated boundary functions, one would also manage to circumvent this clear cause of computational difficulty besides

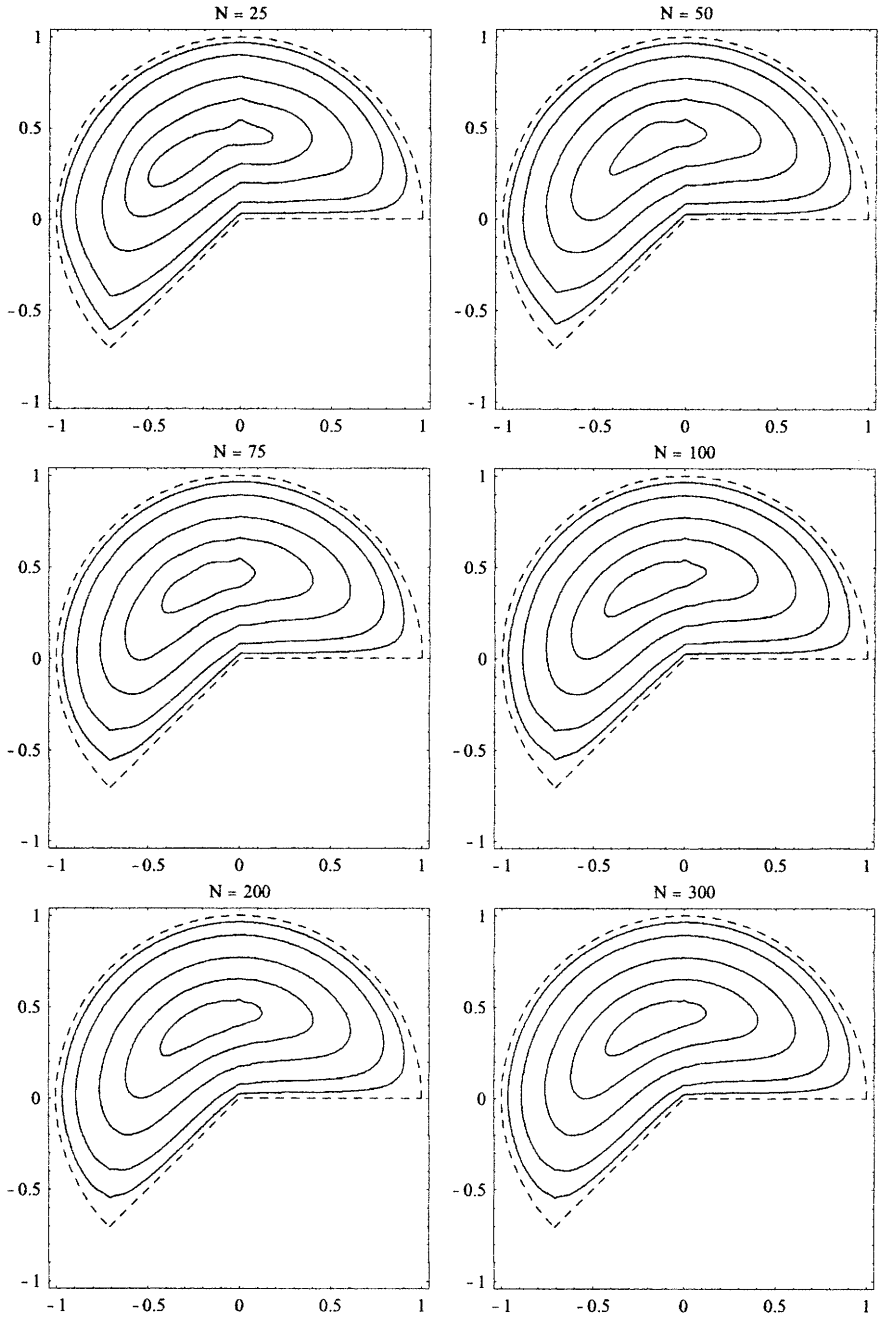

Fig. 2. Graphical convergence of temperature field for $\phi_0 = 225°$, with $\tau = 0.03$

improving the level of interpolation in the domain approximation.

6 Conclusions

A general analytical solution to linear diffusion problems defined within a class of arbitrarily shaped domains was formally derived, by employing ideas from the generalized integral transform technique (GITT). To validate the proposed approach, a solution of a test case problem was undertaken and a comparison of the obtained results with the known exact solution carried out. The current approach is also applicable to the solution of non-linear systems as well, by offering an adequate basis of eigenfunctions.

Moreover, an effort was done towards the flexibilization and performance improvement of the computational solution, by admitting sets of points instead of closed functional forms for the boundary description. These ideas were also validated through a comparison of the test case problem solution in boundary-approximated domains against the equivalent exact boundary-representation.

The present contribution focused on the solution of the associated eigenvalue problem in the arbitrary region via integral transforms. Nevertheless, one must bear in mind that the original diffusion problem presented may also be directly transformed without the requirement of an intermediate stage of eigenquantities computation. In this sense, coupled ordinary differential systems for the

Table 2. Convergence analysis of temperature field for approximate boundary-representation

u_{max}	$N = 25$	$N = 50$	$N = 75$	$N = 100$	$N = 200$	$N = 300$	$N = 400$	$N = 500$
$\phi_0 = 90^\circ$, $\tau = 10^{-2}$, $\phi = 45^\circ$, $R = 1/2$ (Exact solution = 0.974738)								
1	0.965168	0.976061	0.973615	0.972817	0.973387	0.973417	0.973414	0.973307
2	0.976121	0.976773	0.974390	0.974537	0.974247	0.974355	0.974355	0.974573
3	0.977051	0.972537	0.974214	0.974908	0.974882	0.974353	0.974862	0.974592
4	0.974773	0.973919	0.974641	0.975586	0.974923	0.974416	0.974674	0.974691
5	0.972851	0.974361	0.974846	0.974278	0.974492	0.974604	0.974772	0.974568
6	0.972481	0.973947	0.974688	0.974711	0.974970	0.974479	0.974764	0.974594
7	0.972367	0.973931	0.974745	0.974279	0.974930	0.974773	0.974611	0.974816
8	0.976182	0.974072	0.974869	0.974515	0.974686	0.974661	0.974674	0.974698
9	0.975905	0.973819	0.974492	0.974560	0.974912	0.974696	0.974825	0.974700
10	0.976108	0.974087	0.974757	0.974811	0.974747	0.974618	0.974753	0.974772
15	0.975827	0.975504	0.974574	0.974615	0.974520	0.974734	0.974778	0.974693
20	0.975852	0.975560	0.974654	0.974700	0.974582	0.974803	0.974695	0.974724
25	0.975860	0.975582	0.974690	0.974732	0.974616	0.974822	0.974738	0.974743
∞	0.975795	0.975540	0.974677	0.974711	0.974738	0.974768	0.974759	0.974772
$\phi_0 = 90^\circ$, $\tau = 10^{-1.5}$, $\phi = 45^\circ$, $R = 1/2$ (Exact solution = 0.642729)								
1	0.606929	0.606437	0.605353	0.605597	0.605890	0.605933	0.605997	0.605946
2	0.633490	0.635119	0.634856	0.634997	0.634871	0.634744	0.634746	0.634869
3	0.640851	0.638487	0.639026	0.639256	0.639437	0.639218	0.639393	0.639337
4	0.640332	0.640283	0.640837	0.641096	0.640938	0.640753	0.640788	0.640806
5	0.641877	0.641437	0.641630	0.641345	0.641415	0.641375	0.641537	0.641462
6	0.642006	0.641508	0.641842	0.641971	0.642021	0.641753	0.641886	0.641808
7	0.642206	0.641721	0.642097	0.641850	0.642188	0.642148	0.642048	0.642137
8	0.641832	0.642006	0.642381	0.642176	0.642186	0.642230	0.642211	0.642223
9	0.641692	0.641876	0.642147	0.642142	0.642374	0.642344	0.642403	0.642342
10	0.642008	0.642200	0.642470	0.642459	0.642439	0.642357	0.642404	0.642416
15	0.641985	0.642641	0.642473	0.642446	0.642465	0.642526	0.642592	0.642573
20	0.642112	0.642773	0.642609	0.642579	0.642597	0.642656	0.642633	0.642641
25	0.642168	0.642832	0.642671	0.642639	0.642656	0.642707	0.642694	0.642695
∞	0.642194	0.642865	0.642708	0.642672	0.642724	0.642728	0.642728	0.642738
$\phi_0 = 90^\circ$, $\tau = 10^{-2}$, $\phi = 45^\circ$, $R = 3/4$ (Exact solution = 0.910395)								
1	0.849161	0.841066	0.838781	0.839967	0.841618	0.841806	0.841755	0.842230
2	0.891619	0.894875	0.890755	0.891174	0.892615	0.891795	0.891918	0.891982
3	0.903727	0.898388	0.899692	0.902729	0.902261	0.902524	0.902111	0.901991
4	0.908144	0.906868	0.904420	0.905062	0.906361	0.905735	0.906030	0.905815
5	0.914558	0.908126	0.908533	0.908493	0.906584	0.907780	0.907633	0.907495
6	0.915376	0.909193	0.908567	0.908435	0.908135	0.908405	0.908498	0.908248
7	0.915895	0.909823	0.909314	0.908859	0.908558	0.909076	0.908500	0.908882
8	0.913677	0.910105	0.909639	0.908543	0.909325	0.909134	0.909359	0.909515
9	0.913838	0.910335	0.909994	0.909165	0.909745	0.909239	0.909386	0.909627
10	0.913946	0.910529	0.910199	0.909370	0.909611	0.909590	0.909754	0.909612
15	0.914183	0.911370	0.910613	0.909773	0.910179	0.910070	0.910113	0.910078
20	0.914254	0.911504	0.910766	0.910024	0.910329	0.910219	0.910158	0.910206
25	0.914284	0.911564	0.910836	0.910093	0.910399	0.910286	0.910244	0.910280
∞	0.914326	0.911667	0.910961	0.910214	0.910326	0.910313	0.910416	0.910356
$\phi_0 = 90^\circ$, $\tau = 10^{-1.5}$, $\phi = 45^\circ$, $R = 3/4$ (Exact solution = 0.564673)								
1	0.461827	0.458491	0.457741	0.458416	0.459542	0.459608	0.459677	0.459930
2	0.534931	0.537789	0.536135	0.536822	0.537342	0.537195	0.537301	0.537363
3	0.550810	0.549928	0.550489	0.552115	0.552376	0.552638	0.552544	0.552469
4	0.557099	0.557641	0.556586	0.557182	0.557772	0.557789	0.557899	0.557863
5	0.561244	0.559454	0.560144	0.560511	0.559828	0.560298	0.560318	0.560302
6	0.562982	0.561245	0.561061	0.561325	0.561383	0.561604	0.561653	0.561584
7	0.564355	0.562626	0.562568	0.562503	0.562324	0.562571	0.562296	0.562469
8	0.564732	0.562734	0.562677	0.562468	0.562845	0.562829	0.562931	0.563050
9	0.565087	0.563095	0.563124	0.562971	0.563295	0.563179	0.563247	0.563365
10	0.565557	0.563568	0.563600	0.563446	0.563449	0.563473	0.563561	0.563518
15	0.566106	0.564251	0.564170	0.564007	0.564129	0.564111	0.564161	0.564151
20	0.566358	0.564511	0.564431	0.564320	0.564385	0.564370	0.564354	0.564365
25	0.566468	0.564626	0.564547	0.564434	0.564499	0.564480	0.564471	0.564478
∞	0.566654	0.564821	0.564743	0.564629	0.564644	0.564646	0.564671	0.564656

transformed potentials would arise from the integral transformation. These systems are analytically solved for linear transformable problems, and the transformed coefficients given by expressions similar to those presented in this work and therefore the computational procedure may require numerical integration. The integral transform pairs and all transformation process is analogous to the one here presented. It is expected that this path turns out to be competitive against the present one, with respect to the computational effort, in the case of non-linear problems, once coupled ordinary differential systems will arise anyway with both approaches.

Although symbolic computation facilitates the implementation of the presented methodology, the reader should keep in mind that for an optimal scheme, both symbolic manipulation and traditional algorithmic languages (i.e. Fortran, C) can be employed in conjunction.

References

1. **Thompson JF, Soni BK, Weatherill NP** (1999) Handbook of Grid Generation, CRC Press, Boca Raton, FL
2. **Li P, Stagnitti F, Das U** (1996) A new analytical solution for Laplacian porous-media flow with arbitrary boundary shapes and conditions. Mathe. Comp. Mod. 24(10): 3–19
3. **Read WW** (1996) Hillside seepage and the steady water table. I: Theory, Advances in Water Resources, 19(2): 63–67
4. **Ding J, Manglik RM** (1996) Analytical solutions for fully developed flows in double-sine shaped ducts. Heat and Mass Transfer 31: 227–269
5. **Read W, Broadbridge P** (1996) Series solutions for steady unsaturated flow in irregular porous domains. Transport in Porous Media 22: 195–214
6. **Lin JY, Chen H-T** (1997) Hybrid numerical scheme for nonlinear two-dimensional phase change problems with irregular geometry. Heat and Mass Transfer 33: 51–58
7. **Fisher TS, Torrance KE** (2000) Constrained optimal duct shapes for conjugate laminar forced convection. International J. Heat and Mass Transfer 43: 113–126
8. **Tritscher P, Read WW, Broadbridge P, Knight JH** (2001) Steady saturated-unsaturated flow in irregular porus domains. Mathematical and Computer Modelling 34: 177–194
9. **Damean N, Regtien PPL** (2001) Velocity field of the fully developed laminar flow in a hexagonal duct. Sensors and Actuators A 92: 144–151
10. **Cotta RM** (1993) Integral Transforms in Computational Heat and Fluid Flow. CRC Press, Boca Raton, FL
11. **Cotta RM, Mikhailov MD** (1997) Heat Conduction – Lumped Analysis, Integral Transforms. Symbolic Computation. John Wiley & Sons, England
12. **Cotta RM (ed.)** (1998) The Integral Transform Method in Thermal and Fluids Science and Engineering. Begell House, Inc, New York
13. **Cotta RM** (1994) Benchmark results in computational heat and fluid flow – The Integral Transform Method. International J. Heat and Mass Transfer 37(1): 381–394
14. **Aparecido JB, Cotta RM, Ozişik MN** (1989) Analytical solutions to two-dimensional diffusion type problems in irregular geometries. J. Franklin Institute 326: 421–434
15. **Aparecido JB, Cotta RM** (1990) Laminar flow inside hexagonal ducts. Computational Mechanics 6: 93–100
16. **Aparecido JB, Cotta RM** (1990) Analytical solution to parabolic multidimensional diffusion problems within irregulary shaped domains. In: International Conference on Advanced Computational Methods in Heat Transfer, Southhampton, UK, 1: 27–38
17. **Aparecido JB, Cotta RM** (1992) Laminar thermally developing flow inside right triangular ducts. Appl Scientific Research 49: 355–368
18. **Barbuto FAA, Cotta RM** (1997) Integral transformation of elliptic problems within irregular domains – fully developed channel flow. Int. J. Numerical Methods in Heat and Fluid Flow 7(8):778–793
19. **Cotta RM, Ramos R** (1998) Integral transforms in the two-dimensional nonlinear formulation of longitudinal fins with variable profile. Int. J. Numerical Methods in Heat and Fluid Flow 8(1): 27–42
20. **Perez Guerrero JS, Quaresma JNN, Cotta RM** (2000) Simulation of laminar flow inside ducts of irregular geometry using integral transforms. Computational Mechanics 25(4): 413–420
21. **Sphaier LA, Cotta RM** (2000) Integral transform analysis of multidimensional eigenvalue problems within irregular domains. Numerical Heat Transfer, part B – Fundamentals 38: 157–175
22. **Wolfram S** (1999) The Mathematica Book, 4th edn., Wolfram Media/Cambridge University Press, New York/Champaign, IL
23. **Mikhailov MD, Özişik MN** (1984) Unified Analysis and Solutions of Heat and Mass Diffusion. John Wiley & Sons, New York
24. **Mikhailov MD, Cotta RM** (1994) Integral transform method for eigenvalue problems. Communications in Numerical Methods for Engineering 10: 827–835
25. **Sphaier LA** (2000) Integral transformation of diffusion problems within irregular domain: mixed symbolic-numerical computation. MSc thesis, Universidade Federal do Rio de Janeiro – COPPE, Rio de Janeiro, RJ, Brazil
26. **Özişik MN** (1993) Heat Conduction 2nd edn., Wiley Interscience, New York
27. **Mikhailov MD, Cotta RM** (1996) Ordering rules for double and triple eigenseries in the solution of multidimensional heat and fluid flow problems. Int. Communications in Heat and Mass Transfer 23: 299–303